Proc. Of the 10th International Conference on Advances in Engineering, Technology and Management - ICETM 2024

ISBN: 978-1-63248-197-9 DOI : 10.15224/978-1-63248-197-9-07

Finite element simulation of ultra-fine stainless steel wires:Multiscale analysis using crystal plasticity

Naoki Maekawa and Ken-ichi Saitoh

By using finite element method (FEM), we investigate hardening behavior during wiredrawing of ultra-fine stainless steel. To incorporate microstructural changes in polycrystalline grains of austenite stainless steel, slip systems are actually placed in cubic crystal lattice, and a crystal plasticity (CP) FEM analysis is performed. Some parameters (for example, initial hardening rates, and etc.) required in CP-FEM of stainless steel are missing and they are supposed to be difficult to obtain experimentally. Therefore, a series of uni-axial tensile simulations are conducted to determine those parameters which reproduce the experiment. Then, we performed CP-FEM simulations under multi-axial stress conditions corresponding to the wiredrawing condition to investigate the distribution of equivalent strain and stress. The results show that stress and strain tend to decrease towards the surface region, which suggests that hardening behavior in plastic deformation will occur from near the surface.

***Keywords*— Finite element simulation, Wiredrawing, Crystal plasticity, Multi-scale analysis, Stainless steel, Hardening**

I. Introduction

In recent years, the diameter of stainless steel wires for medical use has been substantially reduced, such as in the size less than tens micro-meter [1]. In the manufacturing method using wiredrawing, it is necessary to understand the microscopic changes of material structure. In wiredrawing method, the wire material is subjected to a compression in radial direction and a tension in axial direction. Moreover, shear stress is continuously applied to the wire especially at the outer periphery region by forced contact against the die. Thus, the wire exhibits strong work-hardening behavior during plastic deformation [2]. As the diameter of wire is further reduced to single digit of micro-meter or hundreds of nano-meters, such hardening effect is directly governed by change of microstructure in individual crystal grains and the local hardening becomes much greater than that supposed from averaged plastic strain. Therefore, in this study, crystal plasticity (CP) analysis

Naoki Maekawa
Kansai University
Japan

Ken-ichi Saitoh
Kansai University
Japan

[3] is incorporated to calculate the microstructural change under multi-axial loading which ultra-fine wires will experience during wiredrawing process.

In the CP theory [4], by arranging slip systems in individual crystal grains, local microscopic changes will be considered. The hardening behavior of metallic materials during wiredrawing is supposed to be enhanced by the accumulation of crystal slips at around crystalline defects such as grain boundary and it should be modeled based on polycrystalline arrangement directly implemented by CP theory. Previous researches [3],[5] have reported that physical parameters are significantly affected by crystal orientation and grain size distribution. It was also suggested that, when characteristics in plastic deformation are neatly fitted to experiments and an appropriate constitutive equation which is constructed in advance is used, it is possible to predict the deformation behavior of polycrystalline metals.

Therefore, in this study at first, fitting procedure of material's parameters for stainless steel was progressed. Then, these obtained parameters were implemented into the CP-FEM simulation and the influence of crystal grains under multi-axial stress conditions during wiredrawing was actually investigated. Stainless steel wires are usually drawn multiple of times (each processing is called a "pass") through conical dies with various sizes in order to produce finally ultra-fine wire. This paper will discuss the materials' behavior in representative simulation for one of those passes in wiredrawing.

In this paper, after the introduction of this study is given in Chapter 1, the CP theory and analysis method are explained in Chapter 2, the results and discussion are presented in Chapter 3, and finally the conclusion is given in Chapter 4.

II. Theory and Simulation Method

In this study, the crystal plasticity finite element (CP-FEM) analysis is performed by using an open source software named PRISM-plasticity [4], in which an equation based on the influence of crystal grains is included. So far, various theories of CP have been proposed and some different formulations are found for each. Here, we focus on the CP theory actually integrated in PRISM-plasticity software and an overview is given below.

Considering a microscopic deformation mechanism, the plastic strain rate gradient occurring inside the crystal, $\boldsymbol{L}^{p}$, is

Proc. Of the 10th International Conference on Advances in Engineering, Technology and Management - ICETM 2024

ISBN: 978-1-63248-197-9 DOI : 10.15224/978-1-63248-197-9-07

assumed to be the sum of shear deformations on multiple slip planes, as follows:

$$\boldsymbol{L}^p = \sum_\alpha \dot{\gamma}^\alpha \boldsymbol{S}^\alpha \mathrm{sign}(\tau^\alpha) \quad (\boldsymbol{S}^\alpha = \boldsymbol{m}^\alpha \times \boldsymbol{n}^\alpha) \tag{1}$$

where $\dot{\gamma}^\alpha$ is the shear slip velocity of the slip system α, τ^α is the resolved shear stress acting on slip system α. S^α is the Schmidt tensor defined as follows for the slip system α. $\boldsymbol{m}^\alpha$ and $\boldsymbol{n}^\alpha$ are the slip direction after deformation and the unit normal vector of the slip plane, respectively. The yield surface of each slip system α is defined as follows:

$$f^\alpha = |\tau^\alpha| - s^\alpha \tag{2}$$

where s^α is the slip resistance of the slip system α, and slip occurs when $|\tau^\alpha|$ reaches the critical value, s^α. Furthermore, the change in the slip resistance of the slip system α can be obtained as follows:

$$\dot{s}^\alpha = \sum_\beta h^{\alpha\beta} \dot{\gamma}^\beta \tag{3}$$

where $h^{\alpha\beta}$ is a constant called the hardening rate, which is given by a power law that takes into account the combined effects of work hardening and recovery as follows:

$$h^{\alpha\beta} = \begin{cases} h_0^\beta \left[1 - \frac{s^\beta}{s_s^\beta}\right]^{a^\beta} & \text{if } \alpha = \beta \\ h_0^\beta q \left[1 - \frac{s^\beta}{s_s^\beta}\right]^{a^\beta} & \text{if } \alpha \neq \beta \end{cases} \tag{4}$$

where q is the latent hardening rate, h_0 is the initial hardening rate, s_s is the slip resistance value at the saturated hardening of the slip system. The power factor a^β is a material constant of a^β the slip system β that adjusts the sensitivity of the hardening rate to the slip resistance value.

The material intended for this study is stainless steel and the unit of crystal structure is supposed to be face-centered cubic (fcc). The shape of the simulation model as the representative volume element (RVE) for CP-FEM is a cube with 1.0 mm long sides, and the total number of crystal grains is 32 × 32 × 32 = 32,768. Figure 1 shows the simulation model. The orientation of crystal grains is set randomly (as a prediction, it may be arranged by using experimental data (e.g., EBSD results) in the future). During wiredrawing, plastic deformation occurs in a multi-axial stress state, where radial and circumferential compression, axial tension and at the outer periphery shear stress parallel to longitudinal direction are applied at the same time. Figure 2 shows boundary condition of stress field applied to the cube CP-FEM model and it is compared with a wire drawing model used in conventional FEM simulation.

In addition, data for stainless steel (SUS304) on the initial hardening rate h_0^β, initial slip resistance s_0^β, slip resistance at saturated hardening s_s^β, and power exponent a^β are required. However, in fact, it is difficult to measure these data experimentally. Therefore, in this study, a series of uni-axial tensile simulation [3] with varying these parameters was performed using CP-FEM, and the obtained stress-strain curves were compared with the experimental result of SUS304 to determine the most probable parameters.

As a boundary condition of uni-axial loading test, one of the *x*, *y*, and *z* faces is entirely fixed, and a nominal strain up to 0.081 is gradually applied to the other *x* face. Figure 3 shows the boundary condition for this uni-axial tensile simulation. Table 1 shows input values of Young's modulus, Poisson's ratio, and latent hardening rate, which are thought to be suitable for SUS304. The initial hardening rates are compared for five conditions: h_0^β = 540, 1080, 1620, 2160, 2700 MPa. The initial slip resistance values are compared for four conditions: s_0^β = 64, 112, 160, 208MPa. The slip resistance values at saturated hardening are compared for five conditions: s_s^β = 300, 400, 450, 500, 600 MPa. The power factors are compared for four conditions: a^β = 2.25, 2.50, 2.75, 3.0.

Using four physical parameters for SUS304 determined from above comparison, we analyzed the behavior of plastic deformation in a multi-axial stress state, which is assumed during one pass of wiredrawing process as shown in Figure 2. In this case, as a boundary condition as to the initial cube model, while one side of the *x*-, *y*- or *z*-face is fixed in the *x*-, *y*- or *z*-direction, respectively, different strain rate is applied to the other *x*, *y*, or *z*-faces. The amount of strain applied to each direction along time is shown in Figure 4. By changing the amount of strain rate along the way as shown in Figure 5, an analysis is to be performed taking into account qualitatively the different contact forces in reduction and bearing parts during one pass of wiredrawing process.

Fig.1 Macrostructure of sample CPFEM simulation.

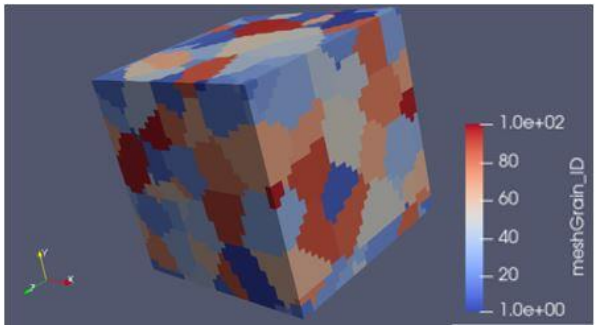

(Different colors are attributed to grains.)

Proc. Of the 10th International Conference on Advances in Engineering, Technology and Management - ICETM 2024

ISBN: 978-1-63248-197-9 DOI : 10.15224/978-1-63248-197-9-07

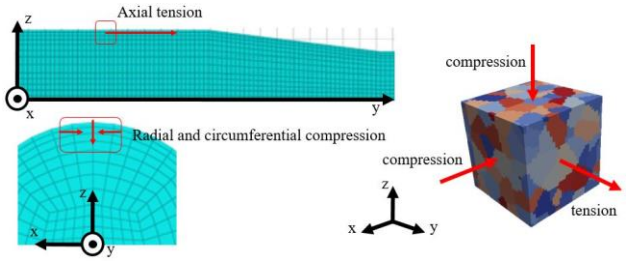

Fig.2 Comparison of stress field in wiredrawing between conventional FEM and crystal plasticity (CP) analysis.

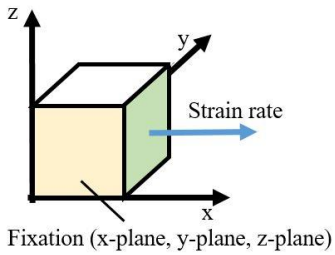

Fig.3 Boundary conditions for uni-axial tensile simulation.

Table 1 Material properties.

Young 's module *E* [GPa]	122
Poisson's ratio [-]	0.3
Latent hardening rate [-]	1.4

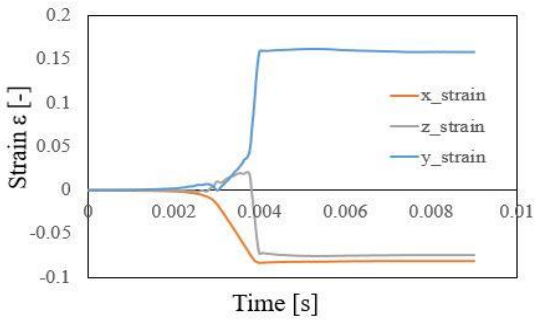

Fig.4 Relation between applied strain in each direction and time.

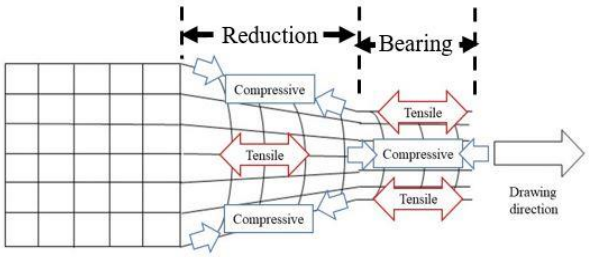

Fig.5 Abstract of stress distribution inside a wire being drawn.

III. Results and Discussion

A. *Comparison of initial hardening rates* (h_0^β)

Figure 6 shows the results of uni-axial simulation comparing stress-strain relations between different initial hardening rates (h_0^β in Eq. (4)). As the initial hardening rate increases, the slope of the stress-strain curve in the plastic region increases. From Eq. (4), it can be understood that the hardening rate and slip resistance values increase with increasing initial hardening rate, which results in the larger slope of stress-strain curves in plastic region and also progresses hardening. Figure 7 shows the relation between initial hardening rate and the slope of the stress-strain curve. The initial hardening rate corresponds to the slope of stress-strain curve just after the yield point. The experimental value of the slope just after yielding for SUS304 is 14,186 MPa [6]. By comparing between the simulated initial hardening rate and the slope of stress-strain curve just after yielding, it is guessed that the initial hardening rate h_0^β for SUS304 comes to be around 2,400 MPa.

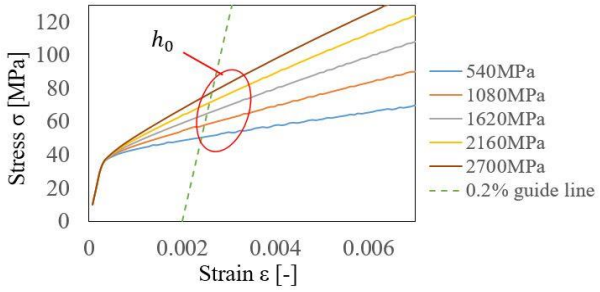

Fig.6 Comparison between initial hardening rates h_0^β.

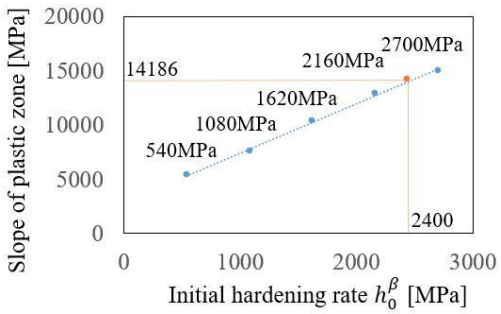

Fig.7 Relation between initial hardening rate h_0^β and slope of stress-strain curve in plastic region.

Proc. Of the 10th International Conference on Advances in Engineering, Technology and Management - ICETM 2024

ISBN: 978-1-63248-197-9 DOI : 10.15224/978-1-63248-197-9-07

B. *Comparison of initial slip resistance values* (s_0^β)

Figure 8 shows the stress-strain curves obtained for different values of the initial slip resistance (s_0^β in Eq. (4)). It is found that the 0.2% proof stress increases in proportion to the initial slip resistance. Figure 9 shows the relation between initial slip resistance and 0.2% proof stress estimated from each stress-strain curves by an offset (guide) line shown in Figure 8. The increase in initial slip resistance is intimately reflected by the yield surface of slip system, and a proportional relationship exists between initial slip resistance and 0.2% proof stress. Where the resolved shear stress exceeds the initial slip resistance, the strain rate increases, and plastic deformation and hardening begin there. The experimental value of 0.2% proof stress for SUS304 is approximately 364 MPa [6]. Therefore, the most probable value of initial slip resistance is chosen as s_0^β = 152 MPa as shown in Figure 9.

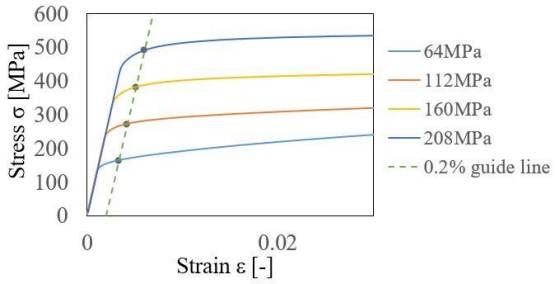

Fig.8 Stress-strain curves comparing between initial slip resistances s_0^β.

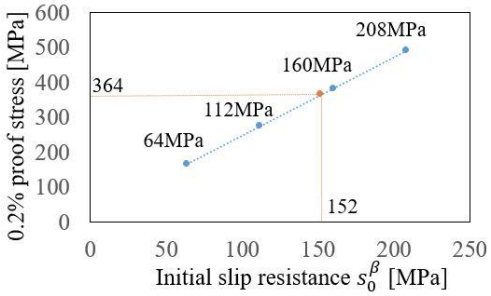

Fig.9 Relation between initial slip resistance s_0^β and the estimated 0.2% proof stress.

C. *Comparison of slip resistance values at hardening saturation* s_s^β

Figure 10 shows the stress-strain curves comparing several different slip resistance values at hardening saturation (s_s^β in Eq. (4)). When s_0^β keeps constant and only s_s^β increases, the slope of stress-strain curve in plastic region increases. The parameter s_s^β is controlling the change of the hardening rate

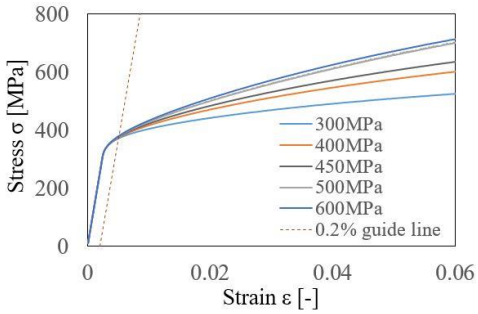

value estimated by Eq. (4). When s_s^β = 450 MPa, the slope of stress-strain curve in the plastic region after initial hardening just matches the experimental value for steel stainless [6].

Fig.10 Stress-strain curves comparing between slip resistance values at hardening saturation s_s^β.

D. *Comparison of powers* a^β

Figure 11 shows stress-strain curves comparing different value of the power factors a^β which is used in Eq. (4). It can be seen that, for larger a^β, the slope of the curves in the plastic region becomes smaller. From Eq. (4), an increase in a^β not so much affects the increase in the hardening rate, and it is thought this parameter has no significant impact on the amount of change in the slip resistance value. It is thought that, as the change in the slip resistance value increases, a saturated state of hardening is more easily reached, and therefore the slope of the plastic region and the value of the work hardening exponent become smaller. Thus, the value a^β = 2.25 can be applied to all slip systems.

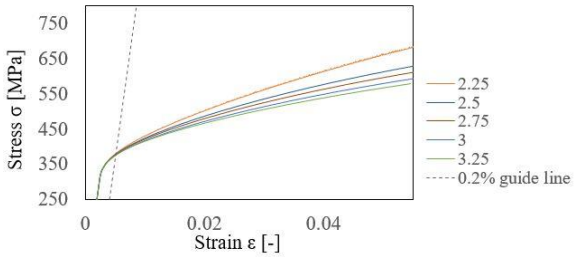

Fig. 11 Stress-strain curves comparing between power factors a^β.

Proc. Of the 10th International Conference on Advances in Engineering, Technology and Management - ICETM 2024

ISBN: 978-1-63248-197-9 DOI : 10.15224/978-1-63248-197-9-07

E. Strain behavior under multi-axial stress

Figure 12 shows the distribution of equivalent stress and equivalent strain (both scalar values) under multi-axial stress assuming wiredrawing process. Figure 12(a) shows a snapshot of calculation model displaying equivalent strain by colors. The shape of the calculation model visibly changed from an initial cube into a rectangular parallelepiped because large plastic strain has been applied in three directions (no shear in this case). As shown in Figure 12(a), linear points along the *z* direction (corresponding to the radial direction of a wire being drawn) are measured. In the calculation model, the coordinate at fixed *z* plane is set to 0, and that of another plane which is applied strain is set to 1. Thus, the graphs in Figure 12 (b) and (c) show the distribution of equivalent stress and equivalent strain from the inside to the outer periphery of the drawn wire material. Figure 12 (b) shows the distribution of equivalent stress and equivalent strain during deformation, and Figure 12 (c) shows those after deformation. It can be seen that both equivalent stress and equivalent strain during deformation tend to enter from the outer periphery but have difficulty to enter into inside. To the contrary, it is observed after deformation that both equivalent stress and equivalent strain have sufficiently entered into the inside region but are reduced near the outer periphery. This is because hardening progresses as strong equivalent strain is applied to the outer periphery during deformation, and ultimately the applied strain is prevented at the outer periphery and then inevitably are consumed in the inside region. Figure 13(a) and (b) show the displacement (y component) at the start and end of the deformation process, respectively. As shown in Fig. 13(a) and (b), plastic deformation of the material is dominated by tensile (positive) stress acting in the drawing direction (y-direction in this model), while the equivalent stress and strain tend to decrease toward the surface region (+z-direction).

In particular, this decreasing trend is obviously seen for strain distribution. This is because strong compressive (minus) stress is always applied to gradually from the outer periphery region during the multi-axial deformation. It is guessed that this effect will proceed a hardening in surface region of the drawn wire. The effect of shear deformation at the surface region is not included in the present model and condition, and it will be discussed in future work.

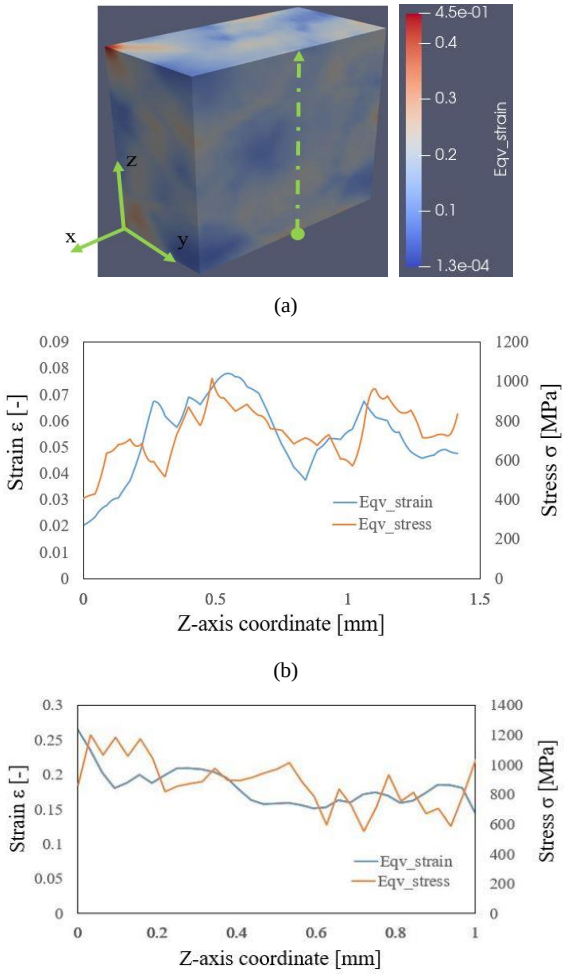

Fig.12 Stress and strain distribution along the direction corresponding to any radial direction of wire: (a) explanation of measuring points, (b) distribution of equivalent stress and equivalent strain during deformation. (c) distribution of equivalent stress and equivalent strain after deformation

Proc. Of the 10th International Conference on Advances in Engineering, Technology and Management - ICETM 2024

ISBN: 978-1-63248-197-9 DOI : 10.15224/978-1-63248-197-9-07

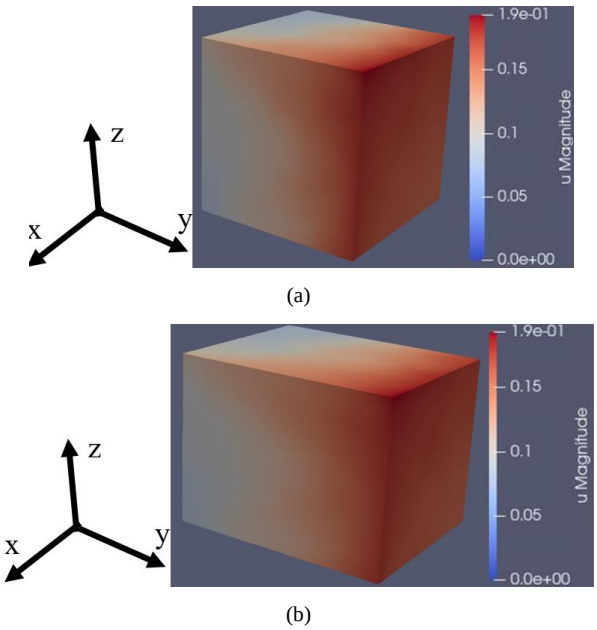

Fig.13 Displacement (y component) distribution under multi-axial loading: (a) at the start of the process, (b) at the end of the process.

IV. Conclusion

In this study, as a preliminary step to the crystal plasticity finite element (CP-FEM) analysis of wiredrawing process of SUS304, some parameters (the initial hardening rate h_0^β, the initial slip resistance value s_0^β, the slip resistance value at hardening saturation s_s^β, and the power exponent a^β) were determined through uni-axial tensile simulation.

It is also understood that those parameters affect somehow total hardening behavior, but are difficult to measure experimentally.

Furthermore, using the CP-FEM incorporating these obtained physical parameters, a new analysis was conducted, in which the condition corresponds to the multi-axial stress state supposedly occurring in wiredrawing process. It was found that strain tends to be enhanced inside rather than the outer periphery region. In actual production, repeated passes of wiredrawing will cause accumulation of work hardening, which will lead to reduction of toughness.

Acknowledgment

This work was supported by JSPS KAKENHI Grant Number 21K03759 (Grant-in-Aid for Scientific Research (C)). One of authors (K.S.) would like to acknowledge and appreciate this support here.

References

[1]. A. Bekmurzayeva, K. Dukenbayev, S. Helena, E. Marsili, D. Tosi, Azevedo and D. Kanayeva, “Optimizing silanization to functionalize stainless steel wire: towards breast cancer stem cell isolation”, Materials, 2020, pp.4-7.

[2]. U. Prisco, “Strain hardening of carbon steel during wire drawing”, materials research, March 2018.

[3]. T. Hama, “Prediction of deformation behavior in magnesium alloy using crystal plasticity finite-element method considering detwinning”, Journal of the Japan institute of light metals, Japan, Vol. 65, No. 5, 2017, pp.178-179.

ISBN: 978-1-63248-197-9 DOI : 10.15224/978-1-63248-197-9-07

[4]. M. Yaghoobi, S. Ganesan, S. Sundar, A. Lakshmanan, , S. Rudraraju , J. Allison, and V. Sundararaghavan, “PRISMS-Plasticity: An open- source crystal plasticity finite element software”, Computational Materials Science 169, 2019.
[5]. M. Men and B. Meng, “Crystal plasticity simulation of yield loci evolution of steel stainless foil”, Materials, 2022.
[6]. Asahi Intecc, Co., Ltd., private communication.